Materials and Structures (2016) 49:3109–3118
DOI 10.1617/s11527-015-0707-2

ORIGINAL ARTICLE

Stabilization of Cr(III) wastes by C_3S and C_3S hydrated matrix: comparison of two incorporation methods

Yang Lv · Xiangguo Li · Geert De Schutter · Baoguo Ma

Received: 2 September 2014 / Accepted: 8 September 2015 / Published online: 10 September 2015

Abstract In the present study, the influence of Cr(III) on the properties of C_3S and its stabilization in C_3S hydrates was investigated by either direct incorporation as Cr_2O_3 during C_3S preparation or introduced as nitrate salt during hydration. Levels of Cr used were from 0.1 to 3.0 wt% of C_3S. The effect of Cr on the polymorph and hydration of C_3S and its immobilization in the hydrates was detected by means of DTA/TG, XRD, isothermal calorimeter and ICP-AES, etc. When doped during sintering process, Cr caused a C_3S polymorph transformation from T1 to T2 and led a decomposition of C_3S into C_2S and CaO resulting in high f-CaO content. Cr doping showed an obvious promotion effect on the hydration properties. The promotion effect decreased when the Cr addition increased to 3.0 wt%. When Cr was added as nitrate salt, Cr showed a retardation effect on the hydration of C_3S due to the formation of $Ca_2Cr(OH)_7{\cdot}3H_2O$, which resulted in a high degree of Cr stabilization.

Y. Lv (✉) · G. De Schutter
Magnel Laboratory for Concrete Research, Department of Structural Engineering, Ghent University, Technologiepark-Zwijnaarde 904, 9052 Ghent, Belgium
e-mail: yang.lv@ugent.be

Y. Lv · X. Li (✉) · B. Ma
State Key Laboratory of Silicate Materials for Architectures, Wuhan University of Technology, Wuhan 430070, Hubei, People's Republic of China
e-mail: lxggroup@163.com

Keywords C_3S · Cr · Polymorph · Hydration · Stabilization

1 Introduction

Disposal of hazardous materials has become a major concern in most industrial countries because they can leach and may contaminate the soil and water with toxic substances, especially for the heavy metal containing wastes. Various technologies have been developed to render a waste non-toxic or to reduce the potential for the release of toxic heavy metals into the environment. Cement based solidification/stabilization (S/S) process is one of the most widely used technologies for safe immobilization of heavy metal containing wastes before their disposal into the environment [1–5]. The immobilization of heavy metal relies on the formation of hydration products. Recently, reusing of heavy metal-contained wastes as raw materials in cement manufacturing has been performed substantially to investigate the stabilization of heavy metal in clinker phases [6–11]. However, to utilize heavy metal-contained waste in cement-manufacturing processes, the effect of heavy metal on the engineering properties of the cement products and environmental aspects must be known.

As a most abundant phase of Ordinary Portland Cement (OPC), alite plays an important role in hydration of cementitious materials. As tricalcium silicate (C_3S) is the pure form of alite, the influence of

heavy metal on the hydration of C_3S can be used to predict the S/S performance of Portland cement.

Chromium(III), a heavy metal of major environmental concern, may cause a serious environmental problem and damage people's health due to its toxic, mutagenic, and carcinogenic nature. Lin et al. [12] studied the solidification/stabilization of chromium with Portland cement and C_3S. Willitsch and Sturm [6] studied the behavior of chromium during the production of cement clinker and the hydration of cement. Chromium(III) was found to be oxidized to Cr^{4+}, Cr^{5+}, and Cr^{6+} during clinkerization at high temperatures. Similar results were also observed by Sinyounga et al. [13]. The mechanism of chromium containment in C_3S during hydration was determined by Omotoso et al. [14]. Stephen et al. [15] studied the influence of Cr and other heavy metals on the properties of doped C_3S. The results showed that all heavy metal only influenced the properties of cement and C_3S when present at much higher loadings than those found in OPC. However, to date there is lack of in-depth report on the impact of Cr on the properties of C_3S during the manufacturing process and hydration. Changes in the properties of C_3S during sintering, hydration and the final leaching process from the hydrates require investigation.

The major purpose of this study is to examine the effect of Cr(III) on the properties of C_3S and its degree of immobilization in C_3S hydrated matrix by comparing two incorporation methods. In the first way, the Cr(III) was introduced in the C_3S solid solution during sintering process mainly to study the effect of Cr(III) on the polymorph of C_3S and the subsequent consequences on hydration properties and immobilization as well. The valorization of Cr was also considered because some heavy metals may affect the sintering property and some of them may evaporate during the sintering process. On the other hand, the Cr(III) was introduced in the C_3S during hydration in the form of nitrate salt to study the effect of Cr on the hydration and also on the environment.

2 Materials and methods

2.1 Preparation of samples

Samples of pure tricalcium silicate (C_3S) were prepared by mixing $Ca(OH)_2$ (analytical grade) and SiO_2 (analytical grade) by a molar ratio of 3:1 in a ball mill for 12 h. The mixtures were pressed and molded into discs forms, and the molded specimens were sintered three times at 1450 °C, each time for 2 h. Between the intervals, the samples were ground and remolded into discs with anhydrous alcohol.

To prepare Cr(III) doped C_3S samples, Cr (introduced as Cr_2O_3) was added to the mixtures of $Ca(OH)_2$ and SiO_2 at 0.1, 0.5, 1.0 and 3.0 wt. % with respect to C_3S and were sintered together according to the process described above. Both the pure and doped C_3S were sintered at 1450 °C for 2 h three times.

The well prepared samples were then ground to particle size <75 μm to be ready for the followed testing process and hydration reaction.

2.2 Hydration reaction

The hydration reactions were carried out by mixing 10 g of each sample with 5 mL de-ionized water (water/C_3S = 0.5). For samples P1–P4 (in which pure C_3S was hydrated in Cr-containing solutions), 0.1, 0.5, 1.0 and 3.0 wt% of Cr(III) ions with respect to C_3S were added to the mixing water in the form of $Cr(NO_3)_3{\cdot}9H_2O$. For samples D1–D4, the prepared C_3S doped with different amount (0.1, 0.5, 1.0 and 3.0 wt%) of Cr(III) was hydrated in de-ionized water. As opposed to other publications, in the present paper all given concentrations refer to the heavy metal Cr instead of the oxide. Table 1 shows the composition of the samples. The samples were kept in plastic screw top bottles at laboratory ambient temperature of around 23 °C. The hydrated samples at certain ages were stopped by Acetone-Ether drying.

2.3 Test methods

For all the following analysis, all samples were ground to pass through a 75 μm sieve.

A NETZSC STA-449C thermogravimetric analyzer was used to determine the sintering reactions in raw mixtures during the sintering process. In an air flux of 20 mL/min, the experiments were conducted at atmospheric pressure and temperature ranging from ambient to 1450 °C under air atmosphere using a heating rate of 10 °C/min, and α-Al_2O_3 as reference. The differential thermal analysis (DTA) and weight loss (TG curve) were recorded as a function of temperature during the heating run.

Table 1 The composition of the samples

Sample no.	Treatment	Cr added concentration (wt%)	Water/C_3S ratio
Control	Pure C_3S hydrated in de-ionized water	0	0.5
P1	Pure C_3S hydrated in Cr^{3+} containing solution	0.1	
P2		0.5	
P3		1.0	
P4		3.0	
D1	Cr doped C_3S hydrated in de-ionized water	0.1	
D2		0.5	
D3		1.0	
D4		3.0	

The added concentration of Cr(III) was taken with respect to C_3S

The free lime (f-CaO) content of pure C_3S and doped C_3S samples were determined by glycerin alcohol method according to Chinese Standard GB176-2008 [16].

The X-ray diffraction (XRD) patterns of doped C_3S and the hydrates were examined by a D/max-IIIA X-ray diffractometer (Rigaku Corporation, Japan), using Cu Kα radiation and a position sensitive detector.

Scanning electron microscopic (SEM) images and energy dispersive X-ray spectra (EDS) were collected with a JEOL JSM-7100F SEM/EDS microscope at an acceleration voltage of 15 kV.

A TAM air isothermal calorimeter (produced by TA America) was employed to determinate the heat liberation rate during the hydration of pure C_3S and doped C_3S. In this test, 5 g C_3S powder and 2.5 g mixing water (liquid/solid ratio 0.5) were mixed in the calorimetric cell.

The heavy metals concentration in C_3S solid solution was determined by inductively coupled plasma atomic emission spectrophotometer (ICP-AES). To prepare the solution for ICP-AES analysis, approximately 0.5 g sample was successively digested by HNO_3, $HClO_4$ and HF acids [7].

The leaching test was carried out on the 28-day hydrated pastes based on Chinese National Standard Solid waste-Extraction procedure for leaching toxicity-Sulphuric acid & nitric acid method (HJ/T 299-2007) [17]. The hydrated samples were crushed and ground to a powder with a particle size <9.5 mm and leached in the extraction solution (pH 3.20 ± 0.05) prepared by mixing sulphuric acid and nitric acid. For each sample, 10 g of hydrated pastes were weighed into polypropylene bottles, and the extraction solution was added at a liquid to solid ratio of 10:1 (L/kg). At the end of extraction, the leachate was filtered with glass-fiber filter paper. The filtrate was then acidified to pH <2 by the addition of 1 M HNO_3 to prevent precipitation of the metal ions. Finally, the concentration of Cr ions in the filtrate solution was determined by ICP-AES.

3 Results and discussion

3.1 Formation of C_3S doped with Cr(III)

3.1.1 Thermal analysis of doped C_3S

Thermal gravimetry/differential thermal analysis (TG/DTA) technique is an effective tool for determining the sintering reactions in raw mixtures during the sintering process. The TG/DTA analyses were conducted on the raw materials of control and D4, and their TG/DTA curves are shown in Fig. 1.

In the case of control sample, the expected endothermic effect between 400 and 600 °C is attributed to the decomposition of $Ca(OH)_2$, resulting in a mass loss in the corresponding temperature range. The following endothermic peak at around 740 °C is attributed to the decomposition of $CaCO_3$, which is formed from the reaction between the ultra-fine $Ca(OH)_2$ powders and CO_2 in the atmosphere during the raw materials preparation. The corresponding mass loss can be observed in the TG curves.

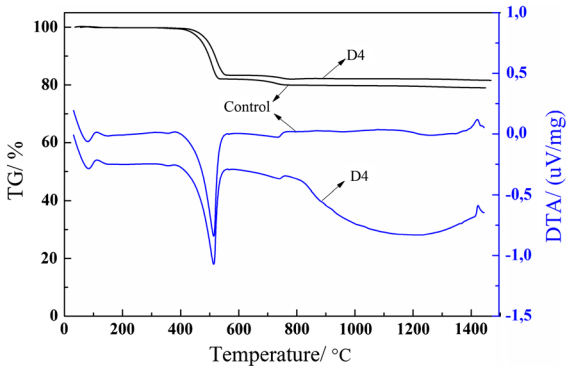

Fig. 1 TG/DTA curves of control and Cr doped C_3S

Comparing with the control sample, the addition of Cr causes no significant differences as far as the temperature of the $Ca(OH)_2$ and $CaCO_3$ decomposition is concerned. TG/DTA curves of D4 are almost the same with those of control sample in these two endothermic effect temperature ranges. The difference in total mass loss between control and D4 is attributed to the addition of Cr (in the form of Cr_2O_3) resulting in a relative lower content of $Ca(OH)_2$ in the raw mixtures of D4 than that of control sample. On the contrary, Cr addition causes a decrease of the formation temperature of liquid phase and an increase of the corresponding peak area. This is due to the formation of an eutectic melt as well as to the higher percentage of the melting material. It is indicated that addition of Cr leads to a lower formation temperature and an increase in quantity of liquid phase. Those changes in the quantity and properties of liquid phase provide a favorable condition for the formation of C_2S and/or C_3S during the sintering process.

3.1.2 XRD patterns

XRD patterns of pure C_3S and doped C_3S are shown in Fig. 2. Peaks appearing between 32° and 33° and between 51° and 52° in XRD profiles of the C_3S are good indicators of the symmetries of the polymorphs [18].

As shown in Fig. 2a, it can be clearly seen that diffraction peaks with respect to dicalcium silicates (C_2S) exist with the Cr addition concentration increasing to 3.0 wt%. It is indicated that the addition of Cr will lead to the decomposition of C_3S into C_2S and CaO. The decomposition of C_3S at higher concentrations of Cr_2O_3 has already been described several times [15, 19, 20].

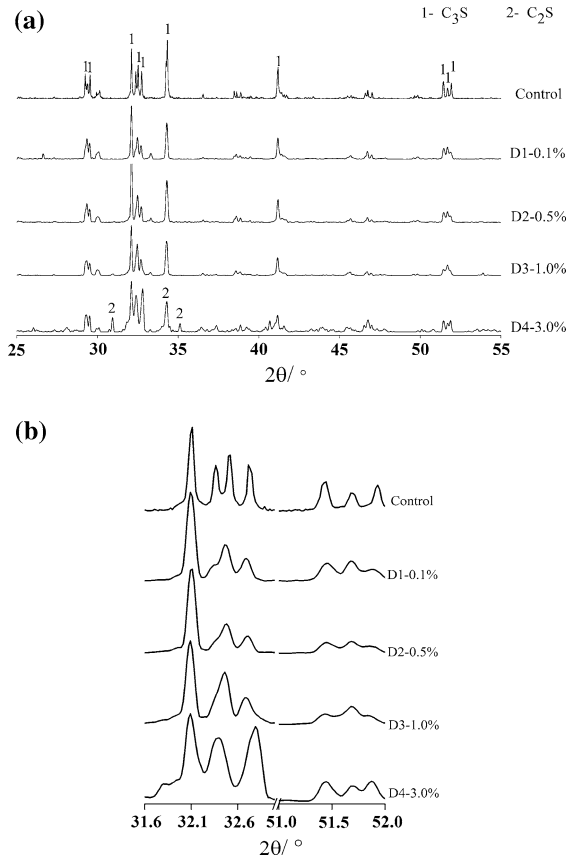

Fig. 2 XRD patterns of doped C_3S. **a** XRD profiles the angles $2\theta = 25°–55°$. **b** XRD profiles of the angles $2\theta = 32°–33°$ and 51°–52°

Details of the XRD patterns of characteristic groups of $2\theta = 32°–33°$ and 51°–52° are given in Fig. 2b. It can be seen that pure C_3S (control) shows a common feature in their XRD patterns with respect to the splitting of peaks from 32° to 33° and 51° to 52°, which are triplets. The addition of Cr (0.5 wt%) causes a transformation from T1 to T2 polymorph. Moreover, with the Cr concentration increasing from 0.5 to 3.0 wt%, no significant changes are found. Different from the results in the present paper, Woermann et al. [21] found no change in the modification of C_3S up to 1.0 wt% Cr, and Stephan et al. [15] found no modification from T1 to T2 until concentration of Cr was up to 2.5 wt%.

3.1.3 f-CaO content

The f-CaO content of pure C_3S and doped C_3S is shown in Fig. 3. The f-CaO content of control sample

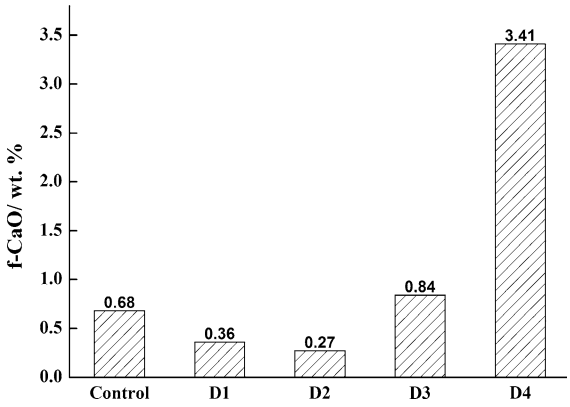

Fig. 3 f-CaO content of doped C_3S

(pure C_3S) is 0.68 wt%. Firstly, the f-CaO content of Cr doped C_3S decreases to 0.27 wt% with the addition of Cr up to a concentration of 0.5 wt%. Then a significant increase in f-CaO content is detected when the Cr added concentration is greater than 1.0 wt%; the f-CaO content raises to 0.84 and 3.41 wt% with Cr added concentration of 1.0 and 3.0 wt%, respectively. The results are in agreement with those of Stephan et al. [15], who found that the f-CaO content decreased with the Cr concentration up to 0.5 wt% then raised to 13.2 wt% with added Cr up to 5.0 wt%. Similar research results were also found by Sychev and Korneev [22], who found a decrease of the f-CaO up to a concentration of 0.7 wt% Cr; with a higher concentration of Cr, the content of f-CaO increased extremely. Different from the results mentioned above, Sakurai et al. [19] found no decrease of f-CaO. Fierens and Verhaegen [20] found no decrease but a linear rise of f-CaO up to 1.2 wt% of Cr; with more Cr they also found an extreme rise of the f-CaO content.

As illustrated in Fig. 1, the addition of Cr can lower the formation temperature and increase the quantity of liquid phase. In other words, Cr doping favors the consumption of CaO and the formation of C_2S and/or C_3S during the sintering process. On the other hand, as shown in Fig. 2, the addition of Cr will lead to the decomposition of C_3S into C_2S and CaO. The synergies of these two effects introduced by Cr doping mentioned above (mineralization and decomposition of C_3S) results in firstly a slight decrease in f-CaO content when the Cr addition increases to 0.5 wt%, and then an extreme increase of f-CaO content of Cr doped C_3S with the Cr addition increases to 3.0 wt%.

3.1.4 SEM

C_3S doped with Cr (1.0 and 3.0 wt%) were analyzed under a scanning electron microscope with energy dispersive X-ray spectra (EDS) to determine the distribution of Cr. Figure 4 shows SEM images of doped C_3S, and the element content of analyzed spots is shown in Table 2. The analyzed results of the selected spots by EDS indicate that the Cr is more likely present in the solid phase with higher silica content, which is mainly C_2S according to the element composition. Cr inhibits the reaction between belite and CaO to form alite but it is not clear whether it is caused by the destabilization of alite or the stabilization of belite [15].

3.1.5 Incorporation of Cr in C_3S

It is well known that doping of C_3S crystal with minor elements will create many defects. According to the hypothesis mentioned by Wang et al. [23], the ion replacement reaction produces only a substitution defect for doping ions of the same valence; whereas for ions of different valence, the ion replacement produces not only a substitution defect but also a vacancy defect or interstitial defect. In the case of substitution solution, the size of ions is a deciding factor for the reaction. When the relative difference in radius of ions is less than 30 %, a substitution solution reaction will take place. However, if greater than 30 %, the substation reaction will not take place.

Although chromium is considered to be present in the C_3S as Cr^{3+}, Cr^{3+} can be oxidized to Cr^{4+}, Cr^{5+}, and Cr^{6+} during clinkerization at high temperature [6, 13]. The ionic radii of Cr^{3+}, Cr^{4+}, Cr^{5+}, Cr^{6+}, Ca^{2+} and Si^{4+} is 0.069, 0.055, 0.049, 0.044, 0.099 and 0.042 nm, respectively. Therefore, the relative difference in ionic radii of Cr (+3, +4, +5 and +6 oxidation state) and Ca^{2+} is greater than 30 %, as well as the relative difference between the ionic radii of Cr (+3, +4) and that of Si^{4+}. The relative difference in ionic radii of Cr (+5, +6) and Si^{4+} is less than 30 %. So according to the hypothesis mention above, a substitution defect would only take place between Cr (+5, +6) and Si^{4+}. In other words, the Si^{4+} could be possibly replaced by Cr^{5+} and/or Cr^{6+}; Cr^{3+}, Cr^{4+} may enter some interstitial sites. However, chromium was found to be present as $CaCrO_4$ in the C_3S doped with Cr [24]. It indicates that only a part of Cr^{6+} plays the role of substitute ions. The formation of any

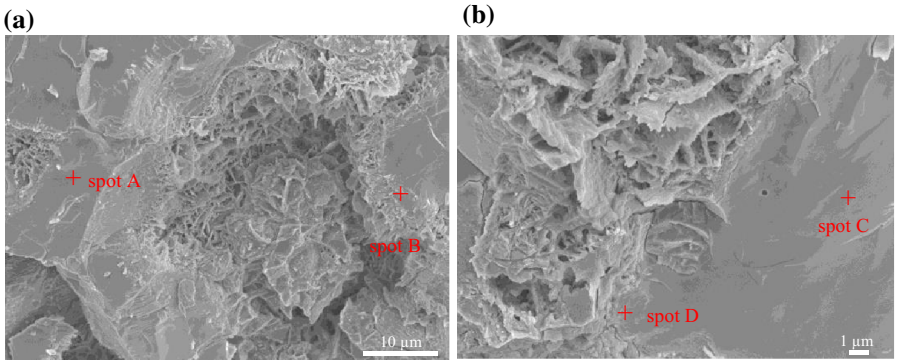

Fig. 4 SEM images of doped C_3S. **a** D3-1.0 %, **b** D4-3.0 %

Table 2 Element analysis measured by EDS

Sample	Cr addition (wt%)	Spot	Element (at.%)			
			Ca	Si	O	Cr
D3	1.0	A	25.49	8.76	65.26	0.49
		B	26.65	12.24	58.42	2.69
D4	3.0	C	26.32	8.57	64.24	0.87
		D	27.26	10.63	57.83	4.28

chromium compound has not been detected in the present study probably due to the less amount.

Besides the substitute hypothesis mentioned above, coupled substitution which do not involve defect or interstitial sites can also occur. The coupled replacement of O^{2-} and Si^{4+} by F^- and Al^{3+} in C_3S was found by Tran et al. [25] in fluoride-mineralized Portland cements. It can be assumed that Ca^{2+} and Si^{4+} might be replaced by two Cr^{3+} ions. Further investigation is necessary to reveal the complex substitution schemes of Cr in C_3S.

3.2 Hydration of pure C_3S and doped C_3S

3.2.1 Hydration of C_3S doped with Cr during the mixing process

XRD patterns of the hydration products obtained from control and P1–P4 compositions are shown in Fig. 5. The main X-ray reflection peaks of unhydrated tricalcium silicate (C_3S) and hydration product portlandite (CH) are identified in the patterns. Although the reflection peak intensity is not directly proportional to the content of crystalline phases, some important information can be obtained from the comparisons of the relative intensity or changes of the intensity with hydration time.

The relative intensities of C_3S peaks of P1-P3 pastes at 1 day are getting weaker than those of the control paste, while the CH peaks are getting stronger. However, the peaks due to CH are not detected in P4 paste. Besides, one reflection peak due to an unknown phase begins to emerge. This phase is not one of the normal hydration products of C_3S.

At 7 days, the relative intensities of C_3S peaks are lower than those of the pastes at 1 day, indicating that hydration has continued with time. Moreover, the relative intensities of CH peaks get stronger, suggesting that more portlandite precipitated. Whereas, there are still no CH peaks emerged in P4 paste. The relative intensity of peak due to an unknown phase emerged at 1 day increases along with the appearance of the other two peaks. This new phase identified by XRD phase analysis is $Ca_2Cr(OH)_7{\cdot}3H_2O$. Chen et al. [1] also found this compound in 14 days hydrates. The results indicate that addition of 3.0 % of Cr^{3+} ions shows an retardation effect on the hydration of C_3S even after 7 days. The retardation may be caused by the formation of $Ca_2Cr(OH)_7{\cdot}3H_2O$. During the early hydration of C_3S in the presence of Cr^{3+}, a slightly soluble calcium salt $Ca_2Cr(OH)_7{\cdot}3H_2O$ is formed in the basic environment from the reaction between Ca^{2+}, OH^- and Cr^{3+}, which consequently reduces the concentration of calcium and hydroxide ions. On one hand, the

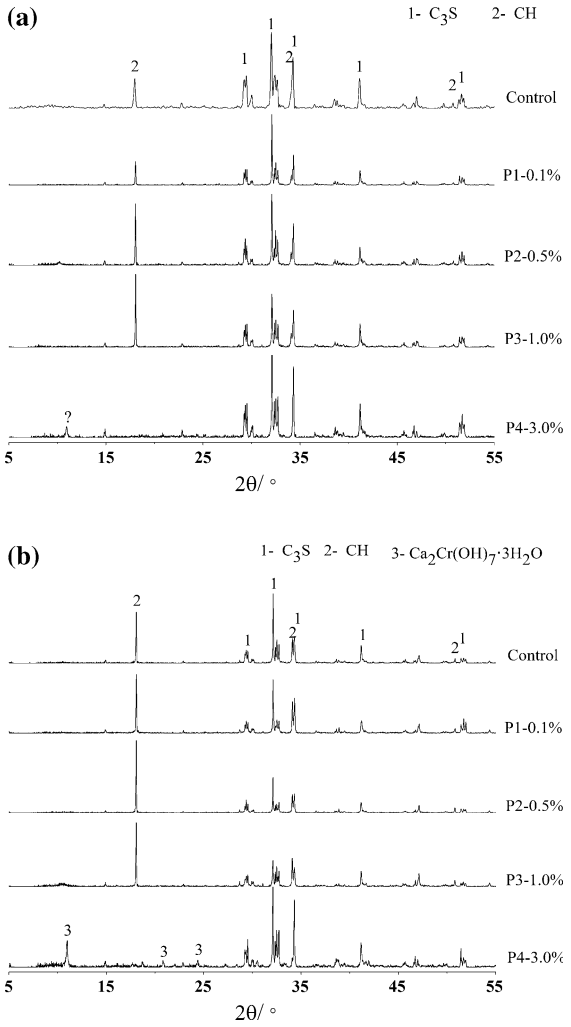

Fig. 5 XRD patterns of pure C_3S hydration in Cr^{3+} ion containing solution. **a** 1 day. **b** 7 days

required supersaturation of the pore solution does not occur until the above formation reaction is completed and, hence, the hydration is delayed. On the other hand, the dissolution of unhydrated C_3S could also be delayed and/or inhibited due to the precipitate of $Ca_2Cr(OH)_7 \cdot 3H_2O$ on the C_3S particles. As a consequence, the hydration is delayed.

3.2.2 *Hydration of C_3S doped with Cr during the sintering process*

The XRD patterns of the hydration products obtained from control and D1–D4 compositions are shown in Fig. 6. The main X-ray reflection peaks of portlandite (CH) and unhydrated tricalcium silicate (C_3S) and dicalcium silicate (C_2S) are identified in the patterns.

The C_3S peaks of the control paste at 1 day are stronger than those of D1–D4 pastes. In D4 paste, the C_2S peaks are still detected due to the low reactivity of C_2S compared with C_3S.

The relative intensities of C_3S peaks of D1-D4 at 7 days pastes are much lower than those of the control paste. Moreover, the CH peaks of D1–D3 pastes are stronger than those of control paste. However, those peaks in D4 paste have almost the same relative intensities as that of control paste. The unhydrated C_2S can still be identified due to its low reactivity. It is implied that Cr doping has a promotion effect on the hydration of doped C_3S, but the promotion effect decreases with the added concentration Cr reaches 3.0 wt%. The promotion effect can also be proved by the results from hydration heat (see detail analysis in Sect. 3.2.3). Similar results were also reported by Stephen et al. [15], in whose study Cr doping was found to accelerate the hydration at the Cr concentrations of 0.5 and 2.5 wt%. The decrease of the promotion effect might be due to the relative low content of C_3S in D4 sample resulting from the decomposition of C_3S into C_2S and CaO induced by Cr doping.

3.2.3 *Rate of hydrating heat liberation*

In order to eliminate the effects of the f-CaO content and the existing of C_2S on the hydration, the heat liberation rate during the hydration was conducted on the samples of P3, D3 (0.84 wt% f-CaO) and control sample (0.68 wt% f-CaO), to determinate the influence of Cr (1.0 wt%) on the hydration of C_3S. The results are shown in Fig. 7.

A rapid heat evolution took place and dropped down within a few minutes. It is the so-called pre-induction period, followed by induction period and acceleration period. During the acceleration period, P3 and D3 show quite different characteristics of heat liberation from control sample. The maximum exothermic rates of P3 and D3 are almost twice of the control sample. Moreover, maximum exothermic rate values of P3 and D3 occur at 10.5 h and 14.0 h, respectively; while the time of maximum exothermic rate of control sample is 9.1 h which is earlier than those of two samples.

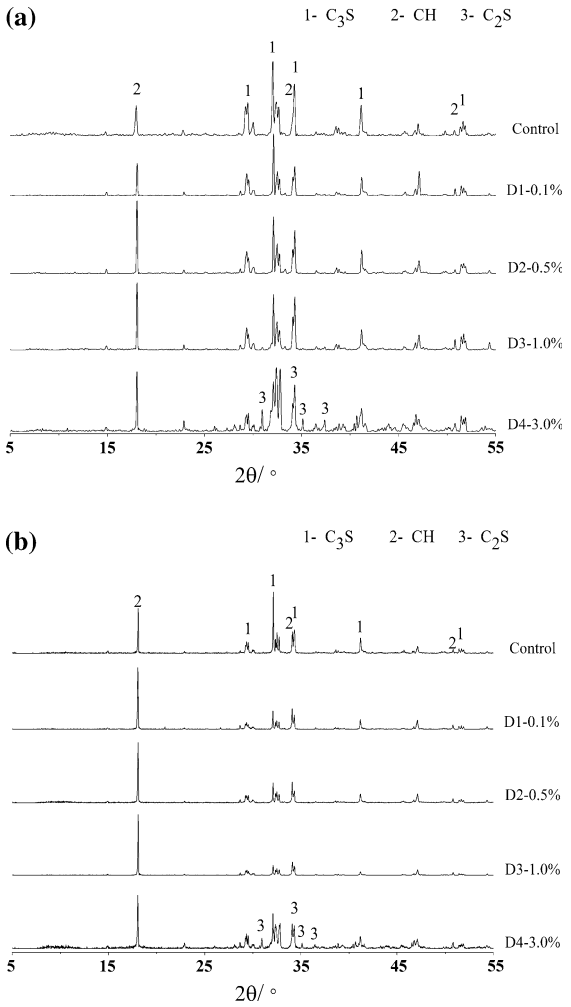

Fig. 6 XRD patterns of doped C_3S hydrates. **a** 1 day. **b** 7 days

Besides, the heat liberation of P3 is characterized by double exothermic peaks during the acceleration period. The double peaks may be attributed to the retardation effect, which caused by the formation of $Ca_2Cr(OH)_7{\cdot}3H_2O$. At the early hydration period, a small amount of this compound is formed and has a negative influence on the hydration representing a drop of heat liberation rate. Soon after that, the rate of heat liberation increases again.

For the D3 sample, the results of hydrating heat liberation obtained in the present study are in accordance with those of Fierens and Verhaegen [20], who observed an increase in the hydrating heat in Cr doped C_3S. According to Fierens and Verhaegen [20], the introduction of Cr_2O_3 into the lattice of C_3S at sufficiently high concentrations can lead to the

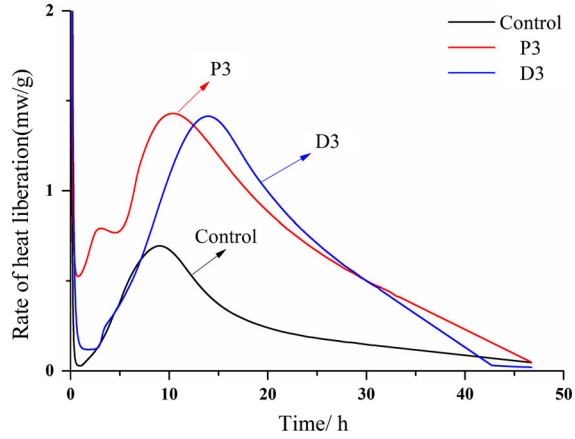

Fig. 7 Curves of the rate of hydrating heat liberation of pure and doped C_3S

appearance of crystal defects; the Cr is distributed at random and produces very reactive sites at high concentrations. Sakurai et al. [19] observed that increased Cr concentration could lead to an increased concentration of screw dislocations. Since these dislocations are potential nucleation sites, reactivity is increased. From the point of crystal chemistry, these circumstances are related to lower stability. The hydration behavior depends directly on the concentration of crystalline imperfections in the phases. Cr doping promotes distortions of the crystalline structure of C_3S. Compared with control sample and P3, a longer induction period was observed in D3 sample. It is related to the rapid hydration of doped C_3S in the pre-induction period which increases the amount of C–S–H and causes the formation of the covering layer on the surface of the particles, which makes the diffusion of ions more difficult and the hydration slower and so it shows a longer induction period. These concepts suggest why the reaction rate of Cr doped C_3S was higher than that of control sample.

3.3 Stabilization of chromium

In order to assess the stabilization properties of Cr in C_3S after sintering for 2 h at 1450 °C for three times, the Cr concentration in the clinker is given in Table 3. The results indicate that the stabilization of Cr in C_3S after sintering is more than 77 % in D3 and D4 sample.

Leaching tests were performed on the 28 days old hydrates according to Chinese National Standard HJ/T 299-2007 [17], which is similar to Toxicity

Table 3 Stabilization of chromium in C_3S and its 28 days old hydrates

Sample	Cr addition (wt%)	Cr concentration in C_3S (wt%)	Leachability of hydrates (mg/L)	GB 5085.3-2007 [24]
P3	1.0	–	0.008	15
P4	3.0	–	0.015	
D3	1.0	0.793	53.7	
D4	3.0	2.324	135.3	

characteristic leaching procedure (TCLP, EPA Method 1311) [26]. The results of leaching test are shown in Table 3.

The leached chromium amount of P3 and P4 is 0.008 and 0.015 mg/L respectively, which is much lower than the permission range of standard value 15 mg/L according to Chinese Standard GB 5085.3-2007 [27]. For the hydrates of doped C_3S, the leaching value is 53.7 and 135.3 mg/L for D3 and D4, respectively; both are much higher than the standard value 15 mg/L. Similar results were obtained by Sinyoung et al. [13], who studied the chromium behavior during cement production; they came to the results that the amounts of leached chromium detected from concrete prepared with the initial (raw meal) chromium concentrations of 1.0, 2.0 and 5.0 % were 46.7, 105.5 and 265.9 mg/L, respectively.

As mentioned before, Cr^{3+} will be oxidized to Cr^{4+}, Cr^{5+}, and Cr^{6+} after high temperature sintering [6, 13]. Sinyoung et al. [13] found Cr species with +3 and +6 oxidation states in the leachate. Cr^{6+} was the predominant species, and the amount leached was close to that of the total chromium content. Cr^{3+} and other species of chromium were leached from the cement at much lower levels than Cr^{6+}. This behavior can be explained by the different solubility of the various chromium species: compounds containing Cr^{4+}, Cr^{5+} exhibit very low solubility, Cr^{3+} compounds are slightly more soluble, and those containing Cr^{6+} show the highest solubility compared to those containing Cr^{3+} [13, 28]. Therefore, Cr^{6+} was found in the leachate at a fraction of approximately 80–90 % of the total Cr. The low solubility of Cr^{3+} containing compounds and the other species in the clinker phases was likely to be the major reason for their low percentage of the total chromium concentration in the control and doped solutions. Consequently, the low leachability of Cr in the P3 and P4 sample can be attributed to the formation of $Ca_2Cr(OH)_7{\cdot}3H_2O$, which is slightly soluble.

4 Conclusion

When doped during the sintering process, addition of up to 0.5 wt% Cr lowers the f-CaO content; then with higher Cr addition (from 1.0 to 3.0 wt%), the f-CaO content raises considerably. The XRD results indicate that addition of Cr will lead to the decomposition of C_3S into C_2S and CaO, resulting in an extreme increase of f-CaO content in Cr doped C_3S. Cr doping could cause a polymorph transformation of C_3S from T1 to T2 with the Cr addition increases from 0.1 to 3.0 wt%.

An obvious promotion effect on the hydration can be observed in the Cr doped C_3S. The promotion effect decreases when the added concentration of Cr increases to 3.0 wt%. While in the case of pure C_3S hydration in Cr^{3+} containing solution, 3.0 wt% of Cr^{3+} ions exhibits a retardation effect on the hydration of C_3S, which may be attributed to the formation of $Ca_2Cr(OH)_7{\cdot}3H_2O$.

Although about 77 % of Cr can be stabilized in the C_3S solid solution in the sintering process, the leaching concentration from the Cr doped C_3S hydrates is higher than the limit. While in the case of pure C_3S hydration in Cr^{3+} containing solution, it shows a high degree of Cr immobilization.

Acknowledgement This work was done in cooperation and with financial support of the National Natural Science Foundation of China (51002110), the Fundamental Research Funds for the Central Universities (2012-IV-025) and State Scholarship Program of China Scholarship Council.

References

1. Chen QY, Hills CD, Tyrer M, Slipper I, Shen HG, Brough A (2007) Characterisation of products of tricalcium silicate hydration in the presence of heavy metals. J Hazard Mater 147:817–825
2. Qiao XC, Poon CS, Cheeseman CR (2007) Investigation into the stabilization/solidification performance of Portland

cement through cement clinker phases. J Hazard Mater 139:238–243
3. Gineys N, Aouad G, Damidot D (2010) Managing trace elements in Portland cement. Part I Interactions between cement paste and heavy metals. Cem Concrete Compos 32:563–570
4. Qian GR, Yang XY, Dong SX, Zhou JZ, Sun Y, Xu YF, Liu Q (2009) Stabilization of chromium-bearing electroplating sludge with MSWI fly ash-based Friedel matrices. J Hazard Mater 165:955–960
5. Batchelor B (2006) Overview of waste stabilization with cement. Waste Manag 26:689–698
6. Willitsch F, Sturm G (2003) Use and preparation of alternative fuels for the cement industry. In: Cement plant environmental handbook. Dorking, pp 151–157
7. Saikia N, Kato S, Kojima T (2007) Production of cement clinkers from municipal solid waste incineration (MSWI) fly ash. Waste Manag 27:1178–1189
8. Pan JR, Huang C, Kuo JJ, Lin SH (2008) Recycling MSWI bottom and fly ash as raw materials for Portland cement. Waste Manag 28:1113–1118
9. Chen HX, Ma XW, Dai HJ (2010) Reuse of water purification sludge as raw material in cement production. Cem Concr Compos 32:436–439
10. Husillos Rodríguez N, Martínez-Ramírez S, Blanco-Varela MT, Guillem M, Puig J, Larrotcha E, Flores J (2011) Evaluation of spray-dried sludge from drinking water treatment plants as a prime material for clinker manufacture. Cem Concr Compos 33:267–275
11. Wu K, Shi HS, De Schutter G, Guo XL, Ye G (2012) Preparation of alinite cement from municipal solid waste incineration fly ash. Cem Concr Compos 34:322–327
12. Lin CK, Chen JN, Lin CC (1997) An NMR, XRD and EDS study of solidification/stabilization of chromium with Portland cement and C_3S. J Hazard Mater 56:21–34
13. Sinyoung S, Songsiriritthigul P, Asavapisit S, Kajitvichyanukul P (2011) Chromium behavior during cement-production processes: a clinkerization, hydration, and leaching study. J Hazard Mater 191:296–305
14. Omotoso OE, Ivey DG, Mikula R (1998) Containment mechanism of trivalent chromium in tricalcium silicate. J Hazard Mater 60:1–28
15. Stephan D, Maleki H, Knofel D, Eber B, Hardtl R (1999) Influence of Cr, Ni and Zn on the properties of pure clinker phases. Part I. C_3S. Cem Concr Res 29:545–552
16. Chinese National Standard (2008) GB176-2008: method for chemical analysis of cement. Chinese Standards Institute (**in Chinese**)
17. Chinese National Standard (2007) HJ/T299-2007: solid waste-extraction procedure for leaching toxicity-Sulphuric acid and nitric acid method. Chinese Standards Institute (**in Chinese**)
18. Bigaré M, Guinier A, Mazie'res C, Regourd M, Yannaquis N, Eysel W, Hahn TH, Woermann E (1967) Polymorphism of tricalcium silicate and its solid solutions. J Am Ceram Soc 50(11):609–619
19. Sakurai T, Sato T, Yoshinaga A (1968) The effect of minor components on the early hydraulic activity of the major phases of Portland cement clinker, vol I. In: 5th ISCC, pp 300–321
20. Fierens P, Verhaegen JP (1972) Structure and reactivity of chromium-doped tricalcium silicate. J Am Ceram Soc 55(6):309–312
21. Woermann E, Hahn Th, Eysel W (1963) Chemical and structural investigations on the solid solutions of tricalcium silicate. Zement-Klak-Gips 16(9):370–375
22. Sychev MM, Korneev VI (1963) Chromalite in Portland cement clinker. translation from: Zhurnal. Prikladnoi Khimii 36:2642–2647
23. Wang S, Li G, Yin C, Lu C (2012) Effect of strontium dioxide on the crystal structure and properties of tricalcium silicate. Adv Cem Res 2496:359–364
24. Katyal NK, Ahluwalia SC, Parkash R (2000) Effect of Cr_2O_3 on the formation of C_3S in $3CaO{:}1SiO_2{:}xCr_2O_3$ system. Cem Concr Res 30:1361–1365
25. Tran TT, Herfort D, Jakobsen HJ, Skibsted J (2009) Site preferences of fluoride guest ions in the calcium silicate phases of Portland cement from $^{29}Si\{^{19}F\}$ CP-REDOR NMR spectroscopy. J Am Chem Soc 131:14170–14171
26. U.S. EPA (1994) Toxicity characteristic leaching procedure (TCLP). 40 CFR 261, Appendix II, US Environmental Protection Agency, Washington DC
27. Chinese National Standard (2007) GB 5085.3-2007: identification standards for hazardous waste-identification for extraction toxicity. Chinese Standards Institute (**in Chinese**)
28. Wang S, Vipulanandan SC (2000) Solidification/stabilization of Cr(VI) with cement: leachability and XRD analyses. Cem Concr Res 30:385–389